JOURNAL OF THERMOPHYSICS AND HEAT TRANSFER
Vol. 12, No. 1, January–March 1998

Development of a Monte Carlo Overlay Method with Application to Spacecraft Glow

Daniel P. Karipides* and Iain D. Boyd†
Cornell University, Ithaca, New York 14853
and
George E. Caledonia‡
Physical Sciences, Inc., Andover, Massachusetts 01810

Brightness calculations for visible emissions from nitrous oxide, known as a spacecraft glow, around the Atmospheric Explorer (AE) satellite are presented over an altitude range of 140–180 km. The flowfield is determined using the direct simulation Monte Carlo method. A novel overlay technique is developed to capture the microscopic behavior of rare atmospheric species, such as nitric oxide. A simple model for glow is proposed, identifying nitric oxide as the important species in the gas phase controlling flow brightness. Sensitivity to altitude and to different chemical reaction cross sections for nitric oxide production is assessed. The importance of nitric oxide production is found to be greatest at lower altitudes. At higher altitudes, the ambient concentration of nitric oxide is the critical factor in determining glow brightness. Comparison of the results with measurements from the AE indicates an efficiency of approximately 0.01 for producing the excited state of nitrous oxide from nitric oxide impacting on the vehicle surface.

Introduction

RAM surfaces in low Earth orbit are known to exhibit visible and uv glow. Such glows have been detected during satellite flights of the Atmospheric Explorer (AE)[1] and Space Shuttle missions.[2,3] In proposed models of this phenomenon, ambient chemical species are assumed to travel through the flowfield without undergoing collisions, and gas-surface reactions are entirely responsible for glow production.[4–9] It is important to focus on two important effects that are critical in the production of glow. At the lower, more dense altitudes, a weak shock forms in front of the ram surface. In this region, the assumption of a collisionless flow is inappropriate. In addition to affecting the physical structure of the flowfield, collisions in the shock can also change the chemical composition. At the higher altitudes, production of precursors to glow, primarily nitric oxide, becomes negligible and the accurate inclusion of freestream concentrations of these precursors is critical. From data taken by the AE satellite, it is evident that the rate at which the brightness of glow at 6563 Å changes with altitude, and therefore, with freestream density, is dramatically different below 160 km, compared to that above 160 km.[1] This experimental evidence suggests that gas–gas collisions become important below 160 km, indicating that the flow is collisional. Therefore, to predict glow brightness accurately, a method is required that includes the effects of 1) gas–gas collisions in the weak shock, 2) precursor ambient species concentrations, and (3) chemical production of the precursors throughout the flowfield.

The freestream conditions at altitudes around 160 km are extremely rarefied. With a Knudsen number of order 100 for the AE vehicle, a high degree of both thermal and chemical nonequilibrium is to be expected throughout the flowfield. The direct simulation Monte Carlo (DSMC) technique is ideal for simulating rarefied flows and has been successfully applied to hypersonic, nonequilibrium aerothermochemistry in previous work.[10] Production of the chemical species critical to the formation of flow in this regime is controlled by rare collisions and chemical events. Proper modeling of such rare events using the DSMC technique requires modifications to the standard form of the method. A new approach is outlined in this paper. In particular, procedures are described for handling the interaction of rare particles with a more dense background flowfield and for calculating the production of particles as a result of rare chemical events. Results are presented for simulation of the AE satellite over a range of altitudes from 140 to 180 km. General flowfield structure, various velocity distributions, and calculations for glow brightness are each discussed.

Note that there is a wealth of data available detailing observed glow around ram surfaces of the Space Shuttle. While there are similarities between AE glow and Shuttle glow, there are also substantial differences in the flow conditions, which could affect the glow production. Available Shuttle data are typically taken in a higher altitude range than AE data, dramatically changing the ambient flow conditions. The control thrusters of the Shuttle also affect the concentration of many chemical species around the ram surfaces. In addition, the surface material of the Shuttle is different than that of the AE satellite, which likely will affect the surface chemistry. Given the additional complexities of simulating Shuttle glow, the present investigation is limited to flow around the AE satellite.

Glow Production Model

A simple model for the glow mechanism is proposed. The production of glow is assumed to be entirely caused by the gas–surface reaction:

$$\mathrm{NO}(g) + \mathrm{O}(a) \rightarrow \mathrm{NO}_2^*(g) \qquad \mathrm{NO}_2^* \rightarrow \mathrm{NO}_2 + h\nu$$

where (g) indicates a molecule in the gas state, and (a) indicates a surface adsorbed particle. The NO_2^* is formed in an excited state and then spontaneously decays to the ground state, emitting a photon. These photons comprise the glow. The molecular surface coverage of a satellite results from a com-

Received Dec. 16, 1996; revision received June 1, 1997; accepted for publication Aug. 5, 1997.

*Graduate Student, Department of Mechanical and Aerospace Engineering. Member AIAA.
†Associate Professor, Department of Mechanical and Aerospace Engineering. Member AIAA.
‡President. Associate Fellow AIAA.

plex balance of atmospheric and flow properties, surface accommodation, thermal desorption, collisional desorption, and chemical reactions. In general, the probability of saturation becomes less likely with increasing altitude. In the present study, the simplifying approximation is made that the surface is saturated with oxygen atoms, one of the dominant ambient species at the altitudes of interest. Obviously, the flux of nitric oxide striking the surface will be crucial to determining the brightness of the glow. Where the flow is collisional, gas–gas collisions and reactions will be important in determining the nitric oxide flux.

A number of simplifying assumptions are made in implementing this model. The assumption of a surface saturated with atomic oxygen is taken to mean that the surface is entirely covered, not just that all available sites are covered. Thus, any NO molecule striking the surface will strike an adsorbed oxygen atom with unit probability. The actual coverage percentage varies with material type and temperature. The actual probability of a reaction between an incident NO molecule and adsorbed oxygen atom is a function of incident energy, surface temperature, physical orientation, and other factors. The only factor included in the present model is the requirement of a sufficient incident energy. Incident NO molecules are required to have a translational energy that exceeds an activation energy for the reaction. Beyond that, the probability of reaction is taken to be unity. Potential additions to the model therefore include a more detailed description of surface chemistry and a variation of the surface coverage of atomic oxygen with altitude. Given the microscopic detail available in a DSMC simulation, the framework exists to readily incorporate these effects.

The proposed kinetic model is quite simplistic and is chosen to emphasize the role of the incident species flux on the surface, these quantities being directly predicted by the present DSMC analysis. Much more complex and competing chemical kinetics may apply. For example, NO may be adsorbed on the surface and oxidized by incoming oxygen atoms. Ambient or flow-produced nitrogen atoms may also interact with the surface, ultimately resulting in NO_2 formation. Chemical reactions on the surface between adsorbed species might also form N_2, O_2, and NO, as well as NO_2. Furthermore, the importance of these reactions may vary with altitude. A study of these surface reactions is not the goal of the present effort. These more complex phenomena may be evaluated in subsequent analyses utilizing the species surface fluxes predicted in the present effort.

For the lower range of altitudes where glow brightness data were taken on the AE (less than 180 km), the ambient concentrations of NO and N are less than the concentrations of N_2, O_2, and O by several orders of magnitude. Furthermore, the rates of the relevant chemical reactions are such that NO and N are not produced in quantity throughout the flowfield. Using the definition that any species with a mole fraction less than 10^{-2} is considered rare and is otherwise considered common, then in all cases considered, NO and N can be classified as rare species, whereas N_2, O_2, and O are common species. Given that the ratio of the number density of the common species to that of the rare species is so great, it is a reasonable assumption that the collisions and reactions of the rare species do not significantly affect the common species flowfield.

Atmospheric Considerations

Flow of air against a ram surface at orbital speed (8 km/s) is primarily a five-species gas mixture, consisting of N_2, O_2, NO, N, and O. Atmospheric concentrations for all of these species excluding NO are determined using the MSIS-90 model.[11] A robust atmospheric model, dependent on a wide variety of specific input conditions, the MSIS model is used here to generate a generic atmosphere. Unfortunately, the number density of nitric oxide is not included in the atmospheric structure produced by the model. Determining accurate NO number densities is a difficult problem. The formation and destruction of nitric oxide is a key component of the odd-nitrogen cycle that occurs in the Earth's atmosphere. Many different factors determine the concentration of NO at any particular time, and the concentration is highly sensitive to many of these factors. In this study, estimates for nitric oxide number densities are taken from experimental rocket measurements.[12] When analyzing the simulation results, it should be kept in mind that only estimates of the NO concentrations have been used. These estimates are likely different from the actual atmospheric NO concentrations experienced during the AE flights.

DSMC Resolution Difficulties

The DSMC technique is particle method applicable to dilute gas flows where binary collisions dominate. Each particle in the simulation represents a large number of real molecules. The ratio of the number of real particles to the number of simulated particles is termed the particle weight W_p. The time step is chosen to be a fraction of the mean collision time of the flow, so that particle motion can be decoupled from the collision mechanics. Simulating rare species and low probability events using the DSMC technique causes a number of resolution difficulties. When simulating a flowfield with one or more rare species, there is often no single acceptable choice for the value of the particle weight. A relatively low value of W_p is required for a statistically significant number of particles representing the rare species to be generated. However, with the particle weight set at such a value, inordinate numbers of particles representing the common species will also be generated. This results in unacceptably high numbers of simulated particles in each cell, requiring massive amounts of computational effort to calculate the flowfield. Alternatively, the value of W_p can be set relatively high, so that reasonable numbers of common species particles are produced. In this case, however, very few, if any, rare species particles are then produced and the simulation no longer generates meaningful statistics for the rare species. Prior experience with rare species and resolution difficulties are discussed in Refs. 13 and 14.

Previous attempts to handle these resolution difficulties have used a continuum-based overlay method.[13,14] A two-step procedure is used to calculate the flowfield. In the first step, a DSMC simulation is performed to determine the properties of the common species throughout the flow domain. The particle weight in this simulation is set so that essentially no rare species particles are created. The second step involves a continuum-based calculation, where mass conservation equations are solved for the rare species using the underlying DSMC flowfield solution as a background. The assumption is made that the behavior of the rare species does not have an appreciable effect on the common species flowfield. This continuum-based approach suffers from two problems. The procedure used to solve the mass conservation equations makes use of the temperature calculated for the common species in each computational cell. However, in the range of altitudes relevant for spacecraft glow, the flowfield is sufficiently rarefied and in such a degree of nonequilibrium that thermodynamic variables such as temperature are not valid representations of the state of the gas. The velocity distribution of the molecules is very often bimodal and certainly not Maxwellian. It is therefore inappropriate to use thermodynamic temperature to characterize the underlying flowfield. In addition to this, the use of a continuum-based overlay also results in a loss of microscopic detail of the rare species. Such detail, particularly velocity distributions, may have a significant impact on chemical rates and glow production. It is important that this microscopic information is retained throughout the simulation.

DSMC Overlay Method

In this study, a DSMC-based overlay technique is developed. Conceptually, this is very similar to the continuum overlay approach, where two separate simulations are performed. In

this case, however, both simulations use the DSMC technique. In the first (base) simulation, the particle weight is set so that the common species are represented at an appropriate level. In the second (overlay) simulation, the particle weight is reduced so that the rare species are represented. Generation of the common species is suppressed during the overlay simulation. In essence, the overlay simulation can be considered to be a magnified simulation, focusing only on the rare species. As a particle method, the DSMC technique is ideal for handling the nonequilibrium nature of the flowfield and for determining the microscopic behavior of the particles. Thus, the DSMC overlay approach overcomes the two main disadvantages of the continuum overlay method.

Coupling Between Rare and Common Species

The main challenge of performing a DSMC overlay simulation lies in achieving a detailed coupling between the two distinct simulations. This is not a concern in the base simulation as it is assumed that the flowfield of the common particles is unaffected by the behavior of the rare particles. It is a significant concern, however, when performing the overlay simulation. The overlay simulation cannot simply be assumed to be a regular DSMC simulation at a lower density. The rare particles are moving through and colliding with a background of much denser common species. In addition, rare chemical events in the base simulation that did not noticeably affect the common species flowfield may have a pronounced affect on the rare species flowfield.

To achieve this coupling, the particle properties are binned in every cell during the sampling period of the base simulation. Five different properties for each species are binned: the three components of velocity, the rotational energy, and the vibrational energy. During the overlay simulation, a temporary common particle is created to act as a collision partner for each rare particle in every cell. These temporary particles have their properties determined through sampling of the bins stored during the base simulation. The binned properties are taken to be statistically independent for this sampling. From these pairs, the appropriate number of common–rare collisons are determined. After standard DSMC collision mechanics are performed, the temporary particles are discarded. Thus, the particles of the overlay simulation interact with the background flowfield at the microscopic level. It is important to note that given the assumption that the rare species have a number density that is several orders of magnitude lower than the common species, the probability of common–rare collisions is much greater than rare–rare collisions. In the cases considered here, rare–rare collisons are neglected in the overlay simulation.

Chemistry in DSMC Overlay

Applying the DSMC overlay procedure outlined in the preceding text to chemically reacting flows is somewhat more involved. It is important to determine which classes of collisions will lead to chemical reactions that affect the rare species. The three possible candidates are common–common collisions, common–rare collisons and rare–rare collisons. As was previously mentioned, rare–rare collision are neglected, so that no reactions stemming from these types of collision are considered. Common–rare collisons are handled using the bins and temporary particles. Standard DSMC reaction routines are used to handle the probability and mechanics of common–rare reactions. After any such reactions, only rare particles remain in the simulation. However, consideration must be given to the relative importance of common–rare reactions compared to the common–common reactions. Because the probability of a common–rare collision is several orders of magnitude lower than a common–common collision, the reaction probability must be very high for the common–rare reaction to be important relative to the common–common reaction. In the cases considered here, the reaction probabilities for the reactions of interest are not sufficiently high, and the inclusion of common–rare reactions has no quantitative effect on the rare species flowfield. This leaves only common–common reactions as the important reactions in terms of the production of rare species.

Common–common reactions cannot be handled during the overlay simulation using standard DSMC techniques because no common–common collision pairs are processed. Regardless of the technique used to determine the concentration and properties of the rare particles created via these reactions, their introduction into the overlay simulation will take the form of a source term for the different rare species in every cell. A more general scheme for accomplishing this would require binning more detailed information, such as velocity distributions of the population of reacting particles, during the base simulation. For the work presented here, an approximate method of determining both the rate of production and the properties of the rare species resulting from common–common reactions is used. The predominant reaction considered is

$$N_2 + O \rightarrow NO + N$$

It is assumed that only the most energetic collisions lead to chemical reaction. In the AE flows, this occurs when a freestream particle collides with a particle that has rebounded from the ram surface of the satellite. Thus, there are two different types of collisions leading to the formation of nitric oxide:

$$\vec{N}_2 + \vec{O} \rightarrow N\vec{O} + \vec{N} \quad (1)$$

$$\vec{N}_2 + \vec{O} \rightarrow N\vec{O} + \vec{N} \quad (2)$$

where the arrows indicate the direction in which the particle is moving. Thus, reaction (1) represents a freestream nitrogen molecule, moving at orbital speed, colliding with an atomic oxygen molecule that has reflected from the surface. Reaction (2) represents freestream atomic oxygen reacting with reflected N_2.

Data on the velocity distributions of O and N_2 scattered from a surface at orbital speeds are limited. Examination of the collision of 8 km/s oxygen atoms with engineering surfaces indicates that the scattering is largely diffuse, although the scattered atoms have a broad velocity distribution centered around 1 km/s.[15] Limited measurements of high-velocity N_2 scattering suggest that the mean scattered velocity is approximately 2 km/s.[16] Using a value of 8 km/s for orbital speed, this results in a relative velocity of 9 or 10 km/s for reactions (1) and (2), respectively. Using these approximations and appropriate values for the cross section of the reaction at these speeds, the rate of production of NO and N can be determined in each cell using the equation:

$$\frac{dn(NO)}{dt} = \frac{dn(N)}{dt} = n(\vec{N}_2)n(\vec{O})g_1\sigma_1 + n(\vec{N}_2)n(\vec{O})g_2\sigma_2$$

where $n(\vec{X})$ represents the number density of species X moving in the direction indicated by the arrow, g is the estimated relative velocity, and σ is the reaction cross section. An appropriate value for σ is found from consideration of other sources. In the first overlay simulation, cross sections of $\sigma_1 = 4 \times 10^{-22}$ m^2 for reaction 1 and $\sigma_2 = 6 \times 10^{-22}$ m^2 for reaction 2 are used.[17] In the other overlay simulation, values for σ_1 and σ_2 obtained from a molecular dynamics trajectory analysis are used[18] and are five times greater than the values used in the first overlay simulation.

In each cell at each time step, a number of NO and N particles are generated according to the production terms evaluated using number densities and velocity distributions from the base simulation. For the nonflow direction components of velocity, the properties of the NO and N particles created can be

approximated from the velocity distributions of N_2 and O, respectively. The velocity component in the direction of the flow for the newly formed NO and N is approximated by the c.m. velocity of the collision, with a thermal spread obtained by sampling the azimuthal velocity distribution in that cell.

Because of the rarefied nature of the atmosphere in the altitude range of interest, the number of collisions predicted and calculated during any DSMC simulation of a body in this environment is quite low. If a particle weighting scheme were to be implemented instead of the overlay method, there would be an insufficient number of N_2, O collisions to create NO particles. This behavior is independent of the numerical values of the weights chosen. Furthermore, the number of collisions throughout the flowfield is sufficiently low, preventing accurate statistics of the velocities of reactant collisions and of NO production to be obtained directly. Thus, there is a need for the general velocity binning and the source term chemistry implementation described earlier.

Results

Simulations are performed at 10-km intervals over the altitude range of 140–180 km for flow over the AE satellite. The geometry of the satellite is approximately a 0.7-m-radius cylinder, 1.0 m in length. At each altitude, three different simulations are made. The first of these is a base DSMC simulation, where the flowfield of the common species is determined and particle properties are binned. Two overlay DSMC simulations are then run using the base simulation for the background conditions. These simulations differ in the choice of cross sections for the source term chemical reactions for NO and N. A summary of freestream values is given in Table 1.

Computational Performance

The simulations presented here are performed using a highly modified version of MONACO, a parallel, object-oriented DSMC code developed at Cornell University.[19] The code is run on up to eight nodes of an IBM SP-2 parallel computer. The total number of particles used during the simulation varies from 1.5×10^5 to 1×10^6, depending on the altitude. The total number of particles is relatively high to ensure that an adequate number of particles exist in the small cells along the axis near the body, and to produce accurate statistical results when binning of the velocity and energy distributions. For the base simulations, the flow takes 6000 time steps to reach steady state, and the flowfield is sampled for 2000 time steps. The transient period for overlay simulations also takes 6000 time steps. For overlay simulations, 5000 sampling steps are used to accurately resolve wall distributions. The computational effort required also varies significantly between the various runs. Base simulations are runs with a computational cost of 10 μs/particle/processor/time step. The additional overhead of sampling the velocity distributions increases the cost to 24 μs/particle/time step in the overlay simulation. This variation in computational cost coupled with the varying number of particles results in a range of execution times from 2 to 10 h.

General Flowfield Structure

A grid consisting of 722 computational cells is used for all altitudes (Fig. 1). Cells of a typical DSMC grid scale in size with the local mean free path of the flow. For the altitudes considered, the freestream mean free path varies from about 3 to 200 m, and thus, is not a useful scaling parameter. Instead, cell sizes are scaled to achieve useful resolutions during sampling. This permits the same grid to be used for all of the altitudes and cases considered.

Table 1 Summary of freestream conditions

h, km	Kn_∞	n_∞(NO), m^{-3}	n_∞(N), m^{-3}
140	27.5	7.0×10^{12}	7.54×10^{12}
150	47.7	5.5×10^{12}	1.39×10^{13}
160	75.9	4.0×10^{12}	2.17×10^{13}
170	114.0	3.0×10^{12}	2.90×10^{13}
180	164.5	2.0×10^{12}	3.44×10^{14}

The overall structure of the flowfield is given in Fig. 2, which shows the translational temperature at 140 km. A diffuse bow shock can be seen in front of the body of the AE, consistent with rarefied, hypersonic flow. No quantitative conclusions should be drawn from plots such as this, as the relevance of thermodynamic variables in this rarefied regime is questionable. It is provided more for a qualitative overview of the structure of the flowfield.

Plots of the number density for all five species along the axis at 140 km and using the first set of reaction cross sections are shown in Fig. 3. The data for these density profiles is obtained from both the base and overlay simulations. The large difference in the number density between the common species and the rare species throughout the entire flowfield is clearly seen. Thus, the definition that a rare species is rare at all points in the flow is valid.

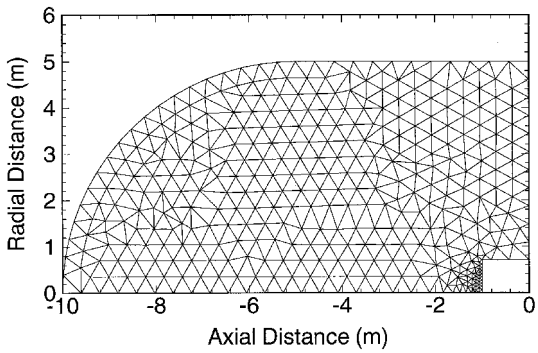

Fig. 1 Computational grid used at all altitudes.

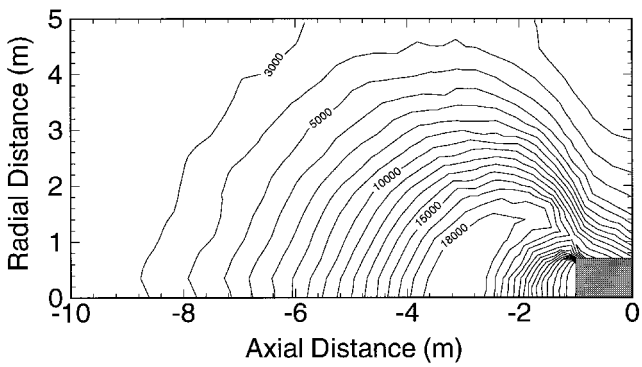

Fig. 2 Common species translational temperature at 140 km.

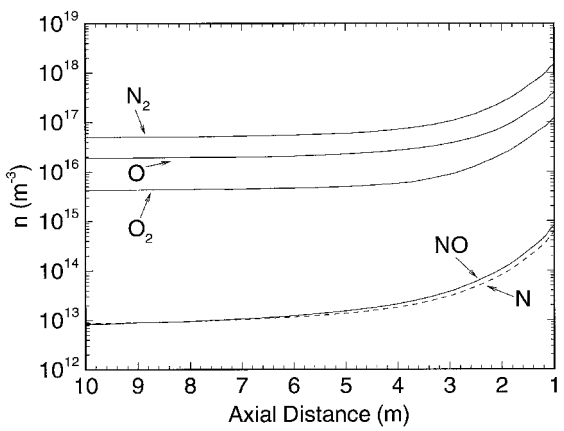

Fig. 3 Number density profiles along the axis at 140 km.

Sensitivity to Altitude

Effects of varying the altitude on the form of the velocity distributions are now considered. For the distributions presented, the comparison is made between cases at 140 and 180 km, using the first reaction cross section. Above this altitude range, the freestream concentration of atomic nitrogen increases to such a level that it can no longer be considered a rare species. Future investigations will consider altitudes above 180 km. Unless otherwise stated, the distributions from the intermediate altitudes follow the trends from lower to higher altitude described in the plots. Note that in all cases, the distributions are normalized. Thus, an increase in one area of a particular distribution must lead to a corresponding decrease in other areas.

Figure 4 illustrates distributions of the normal velocity component of nitric oxide particles impacting the vehicle surface. At 180 km, the majority of the particles striking the surface have a velocity centered around 8 km/s with a thermal spread corresponding to freestream conditions. This peak represents freestream particles that have reached the surface of the satellite without undergoing any collisions. The two other peaks in the 180-km distribution are representative of the nitric oxide particles created from source term reactions. The two distinct peaks are a result of the different c.m. velocities of the two production reactions. The velocity distribution at 140 km shows a similar form. The main distinction lies in the relative importance of the source term NO to freestream NO. At 140 km, the majority of NO particles striking the surface are created in the flowfield, as opposed to those present in the ambient atmosphere. It should also be noted that, because of the importance of the source term chemistry at the lower altitudes, the average velocity of the NO particles hitting the surface is comparatively lower than at the higher altitudes. This is important in interpreting the effect of using the larger reaction cross sections.

The normal velocity distributions have not been plotted for the lower range of velocities ($v_n < 3$ km/s) because the distributions are identically zero in this range. This indicates that the number of common–rare collisions in the flowfield is extremely limited, even at the lowest of the altitudes considered. If there were a substantial number of common–rare collisions, a discernible number of relatively slow-moving NO particles rebounding from the surface would undergo a gas–phase collision and restrike the surface with a low normal velocity component.

Sensitivity of Reaction Cross Sections

Comparison of the effects of the two reaction cross sections tested is most appropriately studied at the lowest altitude considered, 140 km. At this altitude, the base flowfield density is the highest, and therefore, the effects of changing the cross section are the most noticeable. Figures 5–8 compare the nitric oxide x-velocity distributions for cases using the two cross sections at 140 km at four points in the flowfield. The four points chosen are 1) the inflow cell along the axis approximately 10 m from the front of the satellite, 2) a midflowfield cell approximately 3 m from the surface on the axis, 3) the last cell before the wall on the axis, and 4) on the ram surface of the satellite itself.

Figure 5 compares the x-velocity distribution in the inflow cell along the axis. In both cases, two distinct groups of particles are evident. The group with the high, positive x velocity represents freestream particles moving toward the satellite at orbital speeds. The other represents particles that have collided with the front face of the satellite and are moving away with a negative x velocity. Given the extremely rarefied conditions, these particles travel throughout the entire flowfield without undergoing collisions. Note that the relative frequency of particles in the rebounded group is larger with the second, larger cross sections (σ_2). With the larger cross section, more particles are created throughout the flowfield because of the source chemistry. A majority of these particles also collide with the surface, rebound, and are sampled in the inflow cell with a negative x velocity.

A comparison of the x-velocity distributions in the midflowfield cell on the axis is presented in Fig. 6. The two groups evident in the inflow cell are also seen here. The relative increase of the negative x-velocity group with the second cross section is also apparent. In addition to these groups, two smaller groups are distinguishable. Noticeably smaller in magnitude than the first two groups, these can be seen at an x velocity of about 5 km/s. These groups represent the particles created through the source term chemistry that have yet to collide with the AE satellite. The two peaks in this grouping show the difference in the c.m. velocity in the two source term

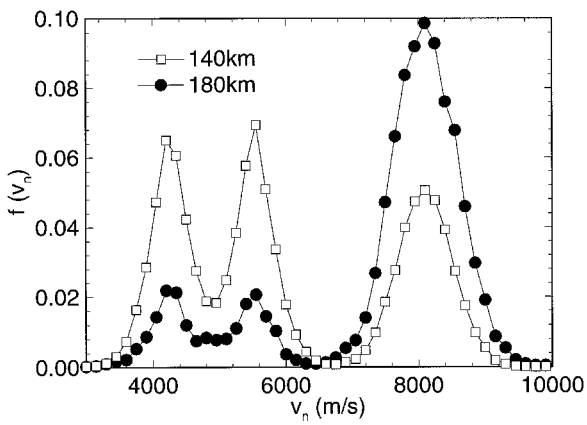

Fig. 4 Variation of the normal velocity distribution functions at the wall with altitude.

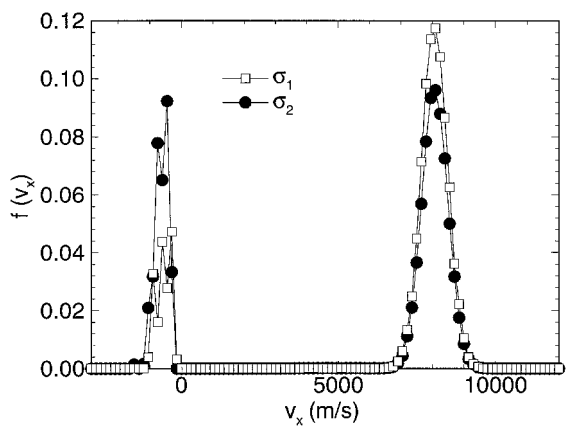

Fig. 5 Variation of the x-velocity distribution functions with cross section in an inflow cell.

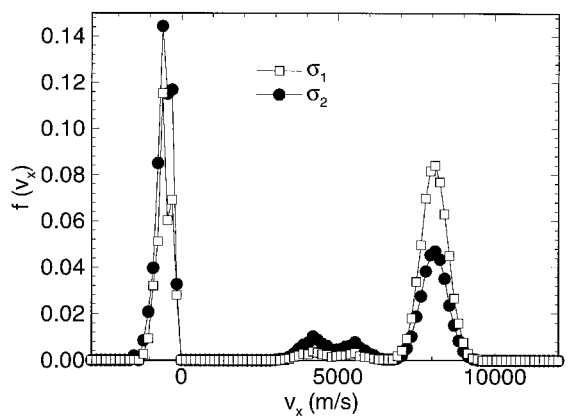

Fig. 6 Variation of the x-velocity distribution functions with cross section in a midflow field cell.

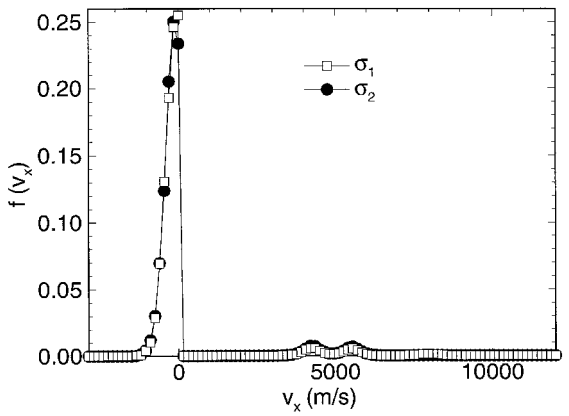

Fig. 7 Variation of the *x*-velocity distribution functions with cross section in a near-wall cell.

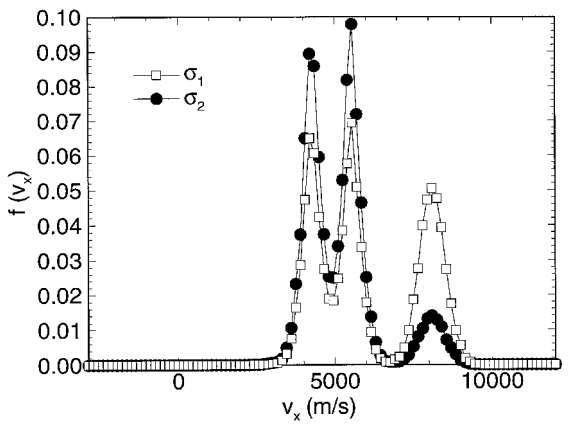

Fig. 8 Variation of the normal velocity distribution functions with cross section at the wall.

reactions. When an N_2 molecule traveling at orbital speed collides with a reflected oxygen atom, the c.m. velocity is larger than when the atomic oxygen is traveling at orbital speed and collides with a reflected N_2 molecule.

Near the wall, the comparison between the distributions is noticeably different. In both cases shown in Fig. 7, the distribution is dominated by a group of reflected particles, moving in the negative x direction with a relatively slow speed. The form of these distributions is consistent with the number density profiles. The magnitude of the velocity of the rebounding particles is relatively small, so that it will take a much longer time for these particles to leave the cell than it will for the high-speed freestream particles in the opposite direction. Consequently, at any time, there are many more reflected particles than freestream particles in cells near the surface. As was noted previously, because of a lack of gas–gas collisions, very few of these particles ever collide and strike the surface again.

The final comparison of the effects of changing the reaction cross section is given in Fig. 8, which shows distributions of the normal velocity component along the vehicle wall. In both distributions, the presence of source term NO as well as freestream NO is evident. Also distinguishable is the bimodal behavior of the source term particles. Once again, the increased importance of the source term chemistry is visible; the distribution obtained using the second set of cross sections is heavily weighted toward these particles. Note that the predominance of source term particles is so large that it greatly overshadows the freestream peak.

Glow Brightness Predictions

Figures 9 and 10 show a comparison between data measured by AE for the glow brightness centered at 6563 Å with a linewidth of 20 Å at varying altitudes[1] and predictions based on the DSMC overlay simulations using the cross-sectional sets σ_1 and σ_2. In both cases, the results have been plotted in units of Rayleighs, where one Rayleigh is defined as 10^6 photons/cm^2/s. The DSMC overlay prediction of the glow brightness is determined through the following procedure. Starting with the average nitric oxide flux striking the surface, it is assumed that each NO molecule striking the surface interacts with an adsorbed oxygen atom. Some experimental evidence suggests that only NO molecules with a translational energy greater than 3 eV may react.[20] Molecules with energy greater than this threshold form a NO_2^* molecule in the gas phase that spontaneously decays, emitting a photon. Note that the effect of this threshold energy is only significant at the lower altitudes, where a significant fraction of the NO is created via chemistry in the weak shock. At orbital speed, ambient NO molecules almost always have an energy greater than the threshold. Inclusion of the threshold in the analysis reduces the lower altitude glow predictions by about factor of 2. Acceptance of the requirement of a threshold energy for reaction is not universal. If an activation energy for reaction is not included in the analysis, the glow brightness predictions at the lower altitudes increase by a factor of 2. Each NO_2^* molecule that is formed is assumed to emit the photon in a random direction, with all directions being equally probable. The wavelength of the photon emitted is determined using the measured laboratory spectrum of nitrous oxide.[21] The DSMC prediction of the brightness is further scaled down so that the prediction agrees with experiment at an altitude of 160 km. The magnitude of this scaling is substantial, on the order of 10^2, and is larger for the second cross-sectional cases. This scaling is required for the most part to correct for the unit probability assumption for the gas-surface reaction. The actual

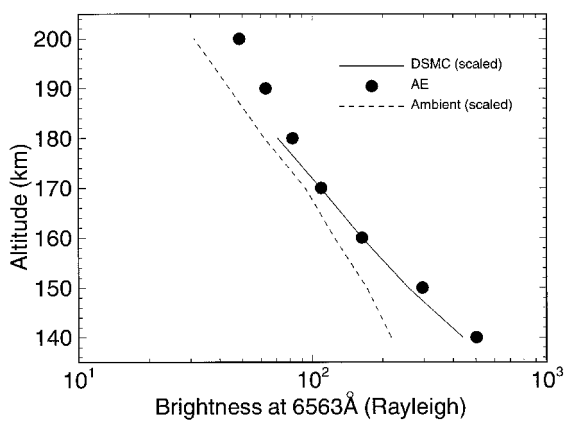

Fig. 9 Comparison of predicted glow brightness using s_1 with AE experimental data.

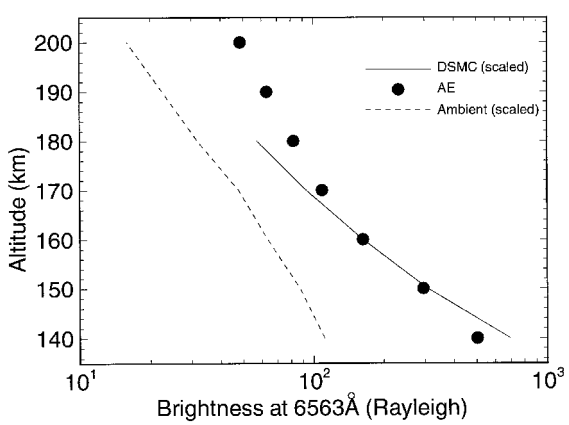

Fig. 10 Comparison of predicted glow brightness using s_2 with AE experimental data.

reaction probability is likely to be significantly less than 1, so that the actual production rate of NO_2^* is less than the incident NO flux striking the surface. In each case, a prediction of the flow brightness using the preceding procedure based solely on freestream nitric oxide is included for comparison. At a particular altitude, the magnitude of the difference between the DSMC overlay prediction and the freestream estimate is an indication of the importance of gas–gas collisions and chemistry.

DSMC glow predictions using the first cross sections are presented in Fig. 9. In general, the predictions show good agreement over the range of altitudes considered. The deviation from the freestream reference is greatest at the lowest altitude. This is consistent with the input conditions and the previous results concerning the production of nitric oxide. At the lower altitudes, the density is higher so the production from source term chemistry is greater. This results in a higher overall NO flux, which in turn, leads to increased glow production. As altitude increases, the DSMC predictions approach the freestream reference predictions. At the highest altitude considered, 180 km, the two predictions almost coincide. This is an indication that production of nitric oxide in the flowfield is unimportant at higher altitudes and that the glow is almost entirely a result of freestream nitric oxide. In addition, it demonstrates the importance of the initial estimates of the nitric oxide densities, as the DSMC predictions will inevitably match the freestream predictions at higher altitudes. Error in the ambient nitric oxide number density directly translates into error in the glow production.

Figure 10 gives the glow predictions from simulations using the second cross sections. The DSMC simulations are seen to overpredict the brightness at the lower altitudes, where the source term production of NO is more important. Larger predicted brightness using the second cross sections is certainly to be expected, as the larger magnitude of the second cross sections results in an increase in the production of NO. It is not entirely clear, however, that the first cross section should be preferred over the second simply on the basis of the superior agreement with the experimental data. Detailed effects of the normal velocity distributions along the wall for the incident nitric oxide are neglected in the simulations presented here. For the lower altitude case, as seen in Fig. 4, a larger fraction of the NO striking the surface is produced through the source term chemistry. This results in the NO striking the surface having a lower average velocity at the lower altitudes. If the simple assumption is made that the higher the incident energy, the higher the probability of reaction, then the predicted brightness at the lower altitudes would be reduced. This will be the focus of further study.

Conclusions

A DSMC overlay technique suitable for simulating rare species has been developed. This method was applied to the flow around the AE satellite to predict the NO_2^* glow brightness over the altitude range of 140–180 km.

Feasibility of the DSMC overlay technique has been demonstrated. Number density profiles shown indicate that the relative difference between the densities of the common and rare species is three orders of magnitude. Thus, the DSMC overlay method can clearly resolve the behavior of rare species. Numerous velocity distributions for nitric oxide have been presented, showing the ability of the method to provide microscopic detail for the rare species throughout the simulation.

Prediction of the glow brightness over a range of altitudes has been made. For the reaction cross sections based on measurement, the qualitative agreement of the scaled predictions with the experiment data was quite good. For the cross sections based on computational chemistry, the agreement was not as good at the lower altitudes where the prediction was significantly larger than experiment. This overprediction could be tempered by the inclusion of collisional energy effects in the formation of NO_2^*. In both cases, the importance of source term chemistry was seen to diminish at higher altitudes. At altitudes greater than 200 km, the results suggest that the glow production is entirely a result of ambient nitric oxide. This highlights the importance of accurately determining the ambient concentrations of the rare species. The computations indicate that the mean efficiency of creating NO_2^* through the impact of NO traveling at orbital speed with a surface saturated with atomic oxygen is approximately 0.01.

Acknowledgments

Funding for this work was provided by the Ballistic Missile Defense Organization under Augmentation Awards for Science and Engineering Research Training award DAAH04-95-1-0204. Computational resources were provided on an IBM SP-2 by the Cornell Theory Center.

References

[1]Yee, J. H., and Abreu, V. J., "Visible Glow Induced by Spacecraft-Environment Interaction," *Geophysical Research Letters*, Vol. 10, No. 2, 1983, pp. 126–129.

[2]Ahmadjian, M., and Jennings, D. E., "Analysis of STS-39 Space Shuttle Glow Measurements," *Journal of Spacecraft and Rockets*, Vol. 32, No. 3, 1995, pp. 507–513.

[3]Swenson, G. R., Rairden, R. L., Jennings, D. E., and Ahmadjian, M., "Vehicle Glow Measurements on Space Shuttle Transportation System Flight 62," *Journal of Spacecraft and Rockets*, Vol. 33, No. 2, 1996, pp. 240–249.

[4]Swenson, G. R., Mende, S. B., and Clifton, K. S., "Ram Vehicle Glow Spectrum; Implications of NO Recombination Continuum," *Geophysical Research Letters*, Vol. 12, No. 2, 1985, pp. 97–100.

[5]Kofsky, I. L., and Barrett, J. I., "Spacecraft Glows from Surface-Catalyzed Reactions," *Planetary Space Science*, Vol. 34, No. 8, 1986, pp. 665–681.

[6]Meyerott, R. E., and Swenson, G. R., "N_2 Spacecraft Glows from $N(^4S)$ Recombination," *Planetary Space Science*, Vol. 39, No. 3, 1991, pp. 469–478.

[7]Greer, W. A. D., Pratt, N. H., and Stark, J. P. W., "Spacecraft Glows and Laboratory Luminescence: Evidence for a Common Reaction Mechanism," *Geophysical Research Letters*, Vol. 20, No. 8, 1993, pp. 731–734.

[8]Green, B. D., Rawlins, W. T., and Marinelli, W. J., "Chemiluminescent Processes Occurring Above Shuttle Surfaces," *Planetary Space Science*, Vol. 34, No. 9, 1986, pp. 879–887.

[9]Caledonia, G. E., Holtzclaw, K. W., Krech, R. H., and Sonnenfroh, D. M., "Mechanistic Investigations of Shuttle Glow," *Journal of Geophysical Research*, Vol. 98, No. A3, 1993, pp. 3725–3730.

[10]Boyd, I. D., Candler, G. V., and Levin, D. A., "Dissociation Modeling in Low Density Hypersonic Flows of Air," *Physics of Fluids*, Vol. 7, No. 7, 1995, pp. 1757–1763.

[11]Hedin, A. E., "The Atmospheric Model in the Region 90 to 2000 km," *Advances in Space Research*, Vol. 8, Nos. 5–6, 1988, pp. 9–25.

[12]McCoy, R. P., "Thermospheric Odd Nitrogen 1. NO, $N(^4S)$, and $O(^3P)$ Densities from Rocket Measurements of the NO δ and γ Bands and the O_2 Herzberg I Bands," *Journal of Geophysical Research*, Vol. 88, No. A4, 1983, pp. 3197–3205.

[13]Boyd, I. D., Karipides, D. P., Candler, G. V., and Levin, D. A., "Effect of Dissociation Modeling in Strongly Nonequilibrium Flows at High Altitude," AIAA Paper 95-0709, Jan. 1995.

[14]Karipides, D. P., Boyd, I. D., and Levin, D. A., "Prediction of Ultraviolet Emissions in Rarefied Hypersonic Flow," AIAA Paper 95-2091, June 1995.

[15]Caledonia, G. E., Krech, R. H., and Oakes, D. B., "Laboratory Studies of Fast Oxygen Atom Interactions with Materials," *European Space Agency (Special Publication)*, Vol. SP-368, 1994, pp. 285–290.

[16]Hurlbut, F. C., "Particle Surface Interaction in the Orbital Context: A Survey," *Rarefied Gas Dynamics*, edited by E. P. Muntz et al., Vol. 116, Progress in Astronautics and Aeronautics, AIAA, Washington, DC, 1989, pp. 419–450.

[17]Upschulte, B. L., Oakes, D. B., Caledonia, G. E., and Blumberg, W. A. M., "Infrared Emissions Arising from the Reactions of Fast $0/0^+$ with N_2," *Geophysical Research Letters*, Vol. 19, No. 10, 1992,

pp. 993–996.
[18]Boyd, I. D., Bose, D., and Candler, G. V., "Monte Carlo Modeling of Nitric Oxide Formation Based on Quasi-Classical Trajectory Calculations," *Physics of Fluids*, Vol. 9, No. 4, 1997, pp. 1162–1170.
[19]Dietrich, S., and Boyd, I. D., "Scalar and Parallel Optimized Implementation of the Direct Simulation Monte Carlo Method," *Journal of Computational Physics*, Vol. 126, No. 2, 1996, pp. 328–342.
[20]Orient, O. J., Martus, K. E., Chutjian, A., and Murad, E., "Recombination of 5-eV $O(^3P)$ Atoms with Surface Adsorbed NO: Spectra and Their Dependence on Surface Material and Temperature," *Physical Review A: General Physics*, Vol. 45, No. 5, 1992, pp. 2998–3003.
[21]Fontijn, A., Meyer, C. B., and Schiff, H. I., "Absolute Quantum Yield Measurements of the NO-O Reaction and Its Use as a Standard for Chemiluminescent Reactions," *Journal of Chemical Physics*, Vol. 40, No. 1, 1964, pp. 64–70.